97C162G
Cask-0.doc

# Tipping Evaluation of Spent Fuel Storage Casks Subjected to Site Specific Earthquake Loading (ISFSI DE) for the Private Fuel Storage Facility

**Rev. 0**
**June 17, 1997**

**Prepared for:**


**Private Fuel Storage, LLC**
**c/o NSP**
**414 Nicollet Mall, RS7**
**Minneapolis, MN 55401**

**Prepared by:**

J.D. Stevenson 6/20/97

**J.D. Stevenson, Consulting Engineer**
**9217 Midwest Avenue**
**Cleveland, OH 44125**
**(216) 587-3808**
**Fax: (216) 662-6273**



9806010115 980519
PDR ADOCK 07200022
B PDR

## Table of Contents

## 1.0 INTRODUCTION

The Private Fuel Storage Facility L.L.C. is currently preparing a 10 CFR Part 72 license application for the Private Fuel Storage Facility (PFSF). Two spent fuel storage cask systems are proposed for use at the PFSF. They are the HI-STORM[1] system designed by Holtec International and the TranStor[2] system designed by Sierra Nuclear Corporation (SNC). Both cask systems are currently under NRC review for generic 10 CFR Part 72 licensing for issuance of Certificate of Compliance. However, the PFSF licensing submittal requires a site specific analysis whereby the casks are shown to not tip over in a seismic event. This purpose of this analysis is to provide the site-specific cask stability analysis. This analysis will bound both spent fuel storage cask systems, since they are very similar in their configuration, size, and weight.

## 2.0 BACKGROUND

Holtec International submitted a site specific evaluation and Sierra Nuclear submitted a generic evaluation of their respective casks to address the various required loadings, which include the concern of tip over during a seismic event. Holtec International performed this analysis using an in-house proprietary program, the details of which were not available. Sierra Nuclear had a generic analysis performed by Advent Engineering Services, Inc. using ANSYS.

### 2.1 Comparison of Casks

Both casks essentially consist of a cylindrical steel inner barrel or basket in which the spent fuel assemblies are placed. This basket is then placed inside a cylindrical concrete shell. Overall dimensions and characteristics of the two casks are shown in Table 2.1.

Table 2.1 -- Overall Dimensional Comparison of Casks[1]

| Cask Vendor | OD (in) | Height (in) | Weight (lb) | c.g. Above Base (in) | Weight x c.g. height (lb-in) |
|---|---|---|---|---|---|
| Holtec Int'l. | 132.5 | 231.25 | 356,521 | 118.0 | $4.2x10^7$ |
| Sierra Nuclear | 136.0 | 222.50 | 309130 | 113.9 | $3.52x10^7$ |

(1) Dimensions of Holtec International cask are from Reference 1. Dimensions for the Sierra Nuclear cask are from Reference 2.

As indicated, the casks are nearly the same in overall dimensions and weight, with the Holtec cask being slightly taller and heavier. Note, the base of the Sierra Nuclear cask is chamfered about 2-3/4", resulting in the base diameter of about 130". Details of the base of the Holtec cask were not provided and were assumed to be uniform. Both types of casks have a steel base.

## 2.2 Description of Advent (Sierra Nuclear Cask) Tipover Analysis

The Advent Tipover analysis was performed using ANSYS (Version 5.1) with a two-dimensional beam element model. Contact elements (STIF52) were used to model the interface between the cask and the basemat. The cask was essentially modeled using rigid beam elements (STIF4), with a single vertical element for the cask, and two horizontal elements at the base to extend to the outer edges of the cask, using an outside diameter of 130 inches. A mass (weight) of 285,000 pounds was included for the cask modeled at an assumed center of gravity of 114 inches above the base. Input motion consisted of a horizontal displacement time-history applied to the center base node of the cask model, and a vertical acceleration time-history applied simultaneously. The model was preloaded with gravity prior to the earthquake loading. Friction effects were included using a coefficient of friction $\mu$ of 0.5.

Note, the displacement loading was applied to the cask model with a constant friction force (lateral resistance at the base of the cask model) active during the full time. This modeling assumption is consistent with that used by Advent. This is a conservative assumption, and tends to overpredict the overturning potential of the cask model.

# 3.0 SOIL-STRUCTURE INTERACTION ANALYSIS

For the purposes of defining the earthquake motion for evaluation of the cask models, soil-structure interaction (SSI) effects were considered. The defined site-specific free field ground surface response spectra, shown in Figure 3.1 and Table 3.1, were assumed applied at the ground surface. Using the computer program SPECTRA,[3] three independent synthetic time-histories were generated (two for the horizontal directions and one for the vertical direction). Total duration was taken as 20 seconds with a trilinear time envelope assumed with a 2 second rise time, 14 second strong motion duration and a 6 second decay time. These time-histories were used as input to the SUPER SASSI/PC program for the SSI analysis.

## 3.1 Soil-Structure Interaction Model

For each basemat, eight casks sit in a rectangular arrangement as shown in Figure 3.2. These basemats are three feet thick and are founded on insitu soil. The upper layer is approximately 30 feet thick and is very soft. The SUPER SASSI/PC program was used to evaluate the SSI. The casks on the basemat were idealized by rigid sticks (beam elements) with translational and rotational inertia concentrated at the c.g. as shown in Figures 3.3 and 3.4. Rigid links were introduced to simulate the physical sizes of the cask bases.

The equivalent soil dynamic properties for best-estimate values are given in Table 3.2. The SSI model was excited by the three acceleration time-histories obtained from SPECTRA. The SSI time history motions computed with SUPER SASSI/PC, shown in Figures 3.5 to 3.12, were used to determine the input motions for the non-linear analyses of the casks. Computed results showed that the rocking motions of the foundation mat were practically negligible in comparison with the

translational motions. The input files for the SUPER SASSI/PC analysis are provided in Appendix A and include the digitized time history motions shown in Figures 3.5 to 3.12.

Based on the NRC requirements in SRP 3.7.1[7] material soil damping was limited to 15 percent (the Geomatrix soil profile has damping up to 19 percent). Three sets of equivalent soil properties were considered: (1) Best Estimate (BE), (2) Half Best Estimate (0.5 BE), and (3) Twice Best Estimate (2 BE). The equivalent damping for 0.5 and 2.0 were adjusted with up to ±20 percent to reflect more properly the effect of damping in the soil degradation basis.

In Figures 3.13 and 3.14 are shown the effective and characteristic amplification of the shallow soft soil layer. It should be noted that prior to lift off, the characteristic frequency of the casks are above 30 Hz which is in the deamplified region. Upon lift off, there is a dramatic shift to a rigid body response below 1.0 Hz which effectively skips the amplified frequency region between 3 and 10 Hz. In Figures 3.15 and 3.16 are resultant response spectra applicable to the base of the casks. It should be noted that below a frequency of about 0.6 Hz the seismic input is below peak ground acceleration values. As can be seen in Section 4.1 of this report, the rigid body responses of these canisters are well below 0.6 Hz.

## 4.0 NON-LINEAR TIPOVER AND RIGID BODY DYNAMICS ANALYSIS OF THE CASK

Several analyses were performed using ANSYS to evaluate the potential for the casks to tip during the seismic event when subjected to Base Mat seismic motions. The models used for these analyses were developed using the Advent concept as the base. In addition, some rigid body dynamic analyses based on Reference 4 were performed to provide insight to the behavior of the ANSYS models, and to evaluate the sliding effects, which were unable to be captured using the ANSYS models.

### 4.1 Rigid Body Dynamics

Response of the casks as fixed-based structures (cantilevers) was estimated to have a fundamental frequency of about 50 Hz. From Reference 4, for a rigid body, excluding the effects of impact, the rocking frequency is dependant on the magnitude of rotation (lift off) at the base. The frequency response drops dramatically with only slight uplift. For example, the rigid body rocking frequency is about 0.33 Hz at 2 degrees, 0.144 Hz at 1 degree, and 0.049 Hz at 7 degrees. At the point where the cask would tipover (approximately 28.85 degrees), the frequency is essentially zero. Just prior to that point at 28 degrees, a frequency response of 0.009 Hz is indicated.

Figures 4.1 and 4.2 show the effect of the impact and no impact respectively, on the rigid body rocking of the cask. Impact is defined for this report as the cask returning to a perpendicular position from a tip up position and contacting the basemat. An initial displaced (rotation) angle of 10 degrees was assumed for the cask (as a rigid body) with the cask then "released". As can be seen, impact effects produce a drastic reduction of the amplitude and frequency response of

the rocking motion.

Figure 4.3 shows the rigid body response of the cask subjected to horizontal and vertical earthquake motion components, assuming no impact effects (very conservative). The maximum rotation angle is about 1.2 degrees.

Figures 4.4 and 4.5 show the rigid body sliding response (no overturning effects) of the cask subjected to the horizontal and vertical earthquake motion components. The maximum sliding distance obtained is less than one foot.

Based on these evaluations, it is concluded that the ANSYS model results appear to be very conservative. The program has limitations in capabilities to model rigid body dynamic effects. The ANSYS models do not directly include impacts and the associated energy loss which results in underestimation of the effects of frequency changes and effective damping which lead to an over estimation of the tipping phenomenon.

## 4.2 ANSYS Non-Linear Time-History Analysis

Using the model developed by Advent as the basis, modifications were made to account for the greater weight and higher center of gravity of the Holtec cask. The base dimension was kept at 130 inches for an effective outside diameter. The model was also extended to three dimensions, modeling the base with rigid beam elements at 30 degree intervals. Analyses were performed using both two-dimensional and three-dimensional models.

Input to the models consisted of horizontal displacement time-histories and vertical acceleration time-histories, similar to the Advent analysis. Gravity effects were included prior to imposing the earthquake motions.

Like the Advent analysis, it was necessary to apply the displacement time-histories to the base of the cask model only. Convergence difficulties precluded applying these motions to the base only, and to the base and cask model simultaneously. By applying the motion to the base only, sliding effects would have been included. By applying the motion to the base and model simultaneously, the effects of the constant friction resistance would have been precluded which results in an overestimation of the overturning effect.

From the best estimate soil properties analyses performed, it was found that the most conservative results (and therefore the greatest overturning response) were obtained with the two-dimensional model with the displacement motion applied only at the center base node of the model. The results of this analysis indicate that the maximum rotation at the base of the cask model is approximately 7.2 degrees. For the three-dimensional model, a maximum rotation of about 1.3 degrees was obtained. Note, for the three-dimensional model, two components of displacement loading were applied simultaneously.

It should be noted that the ANSYS analyses performed did not include effects of sliding or impact. First, this is conservative in that the energy taken up in sliding would reduce the energy associated with tip over. Secondly, it is also conservative because the ANSYS program is not capable of capturing the impact effects directly, nor the large non-linearity involved due to the drastic dependence of frequency with the rigid body rocking amplitude. Further, the use of viscous dampers in ANSYS could be used, although with care, to simulate the energy loss through impacts, but was not done here.

## 5.0 CONCLUSIONS

From the analyses performed as described above, it is concluded that neither Sierra Nuclear nor Holtec casks will tip over during the defined site-specific seismic event.

The model used does not simultaneously evaluate sliding, impact, and rolling effects along with tip-up. In my opinion their inclusion would result in less potential for overturning than that calculated by use of the ANSYS program.

A conservative upper bound lift off rotation of the cask based on the ANSYS analysis which ignores the beneficial effects of impact was found to be 7.2 degrees for best estimate soil properties. This compares to the rotation necessary for overturning of 28.85 degrees.

6.0 REFERENCES

(1) HI-STORM TSAR, Report HI-951312, Rev. 1, January 1997, pages 1.2-1, 3.2-2, and 3.2-5.

(2) SAR - TranStor Storage Cask, Docket No. 72-1023, Revision A, May 1996, pages 1-16, 1-17, and 3-3.

(3) "SPECTRA 2.0 User's Manual," Stevenson & Associates, 1992.

(4) G.W. Housner, "The Behavior of Inverted Pendulum Structures During Earthquakes," Bulletin of the Seismological Society of America, Vol. 53, No. 2, pp. 403-417, February 1963.

(5) "ANSYS User's Manual for Revision 5.0," ANSYS, Inc. (formerly Swanson Analysis Systems), Houston, PA, 1994.

(6) "SUPER SASSI/PC User's Manual," Stevenson & Associates, 1996

(7) USNRC Report NUREG-0800, "Standard Review Plan -- LWR Edition" Sections 3.7.1 and 3.7.2, Rev. 2, August 1989.

(8) Fax Transmittal, from S. Macie, Stone and Webster, to J. Stevenson, JD Stevenson Consulting Engineer, re: PSFS Cask Analysis, transmitting portions of pad drawing (Dwg. 0599601-EC-1 B), May 22, 1997.

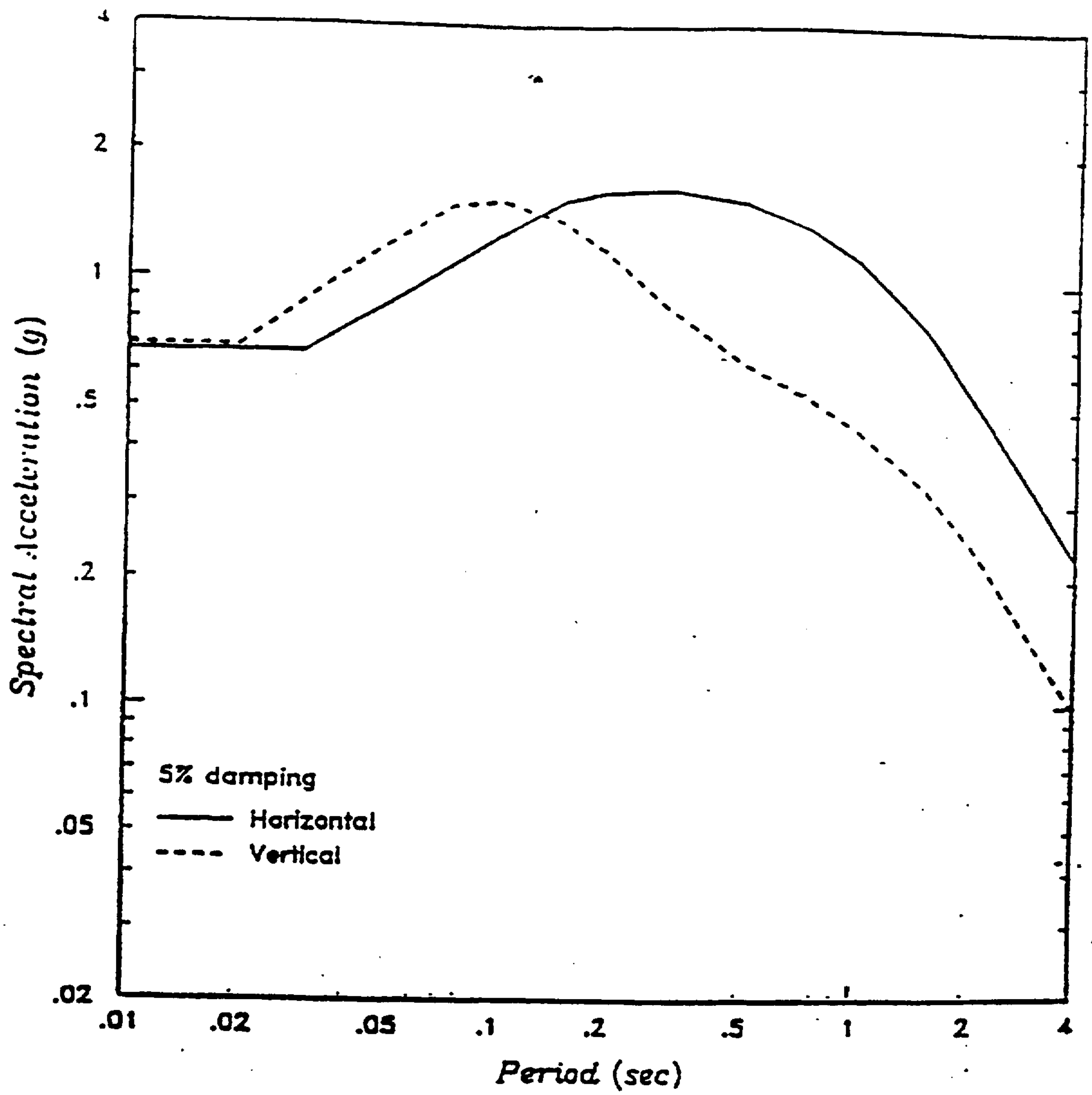


Recommended envelope 84th percentile response spectra

FIGURE 3.1

SWEC #0399601-001
GMX #3801-1 (REV. 0)

49

FIGURE 3.2

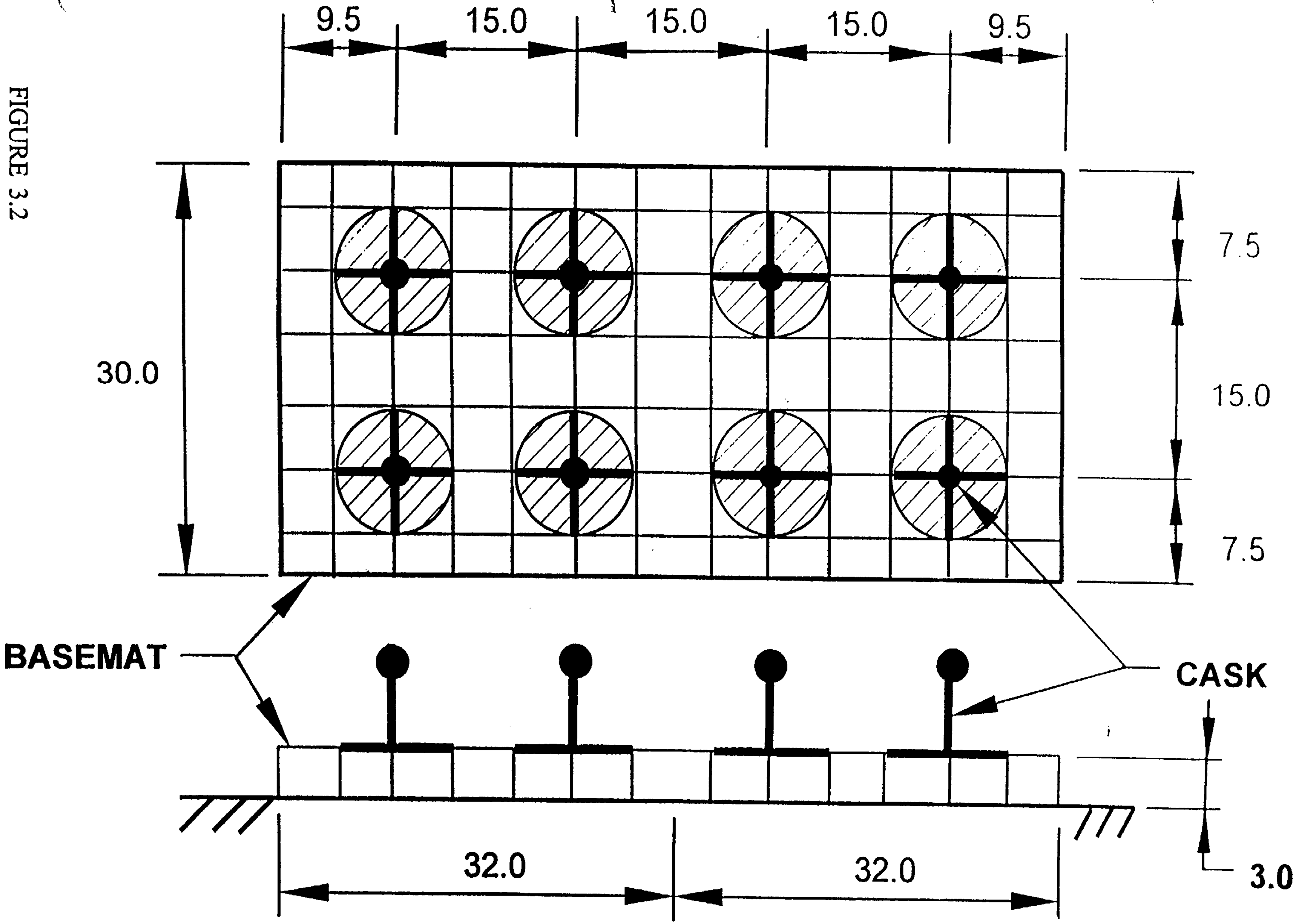


FIGURE : SUPER SASSI SOIL-STRUCTURE INTERACTION MODEL

# HOLTEC CASK MODEL

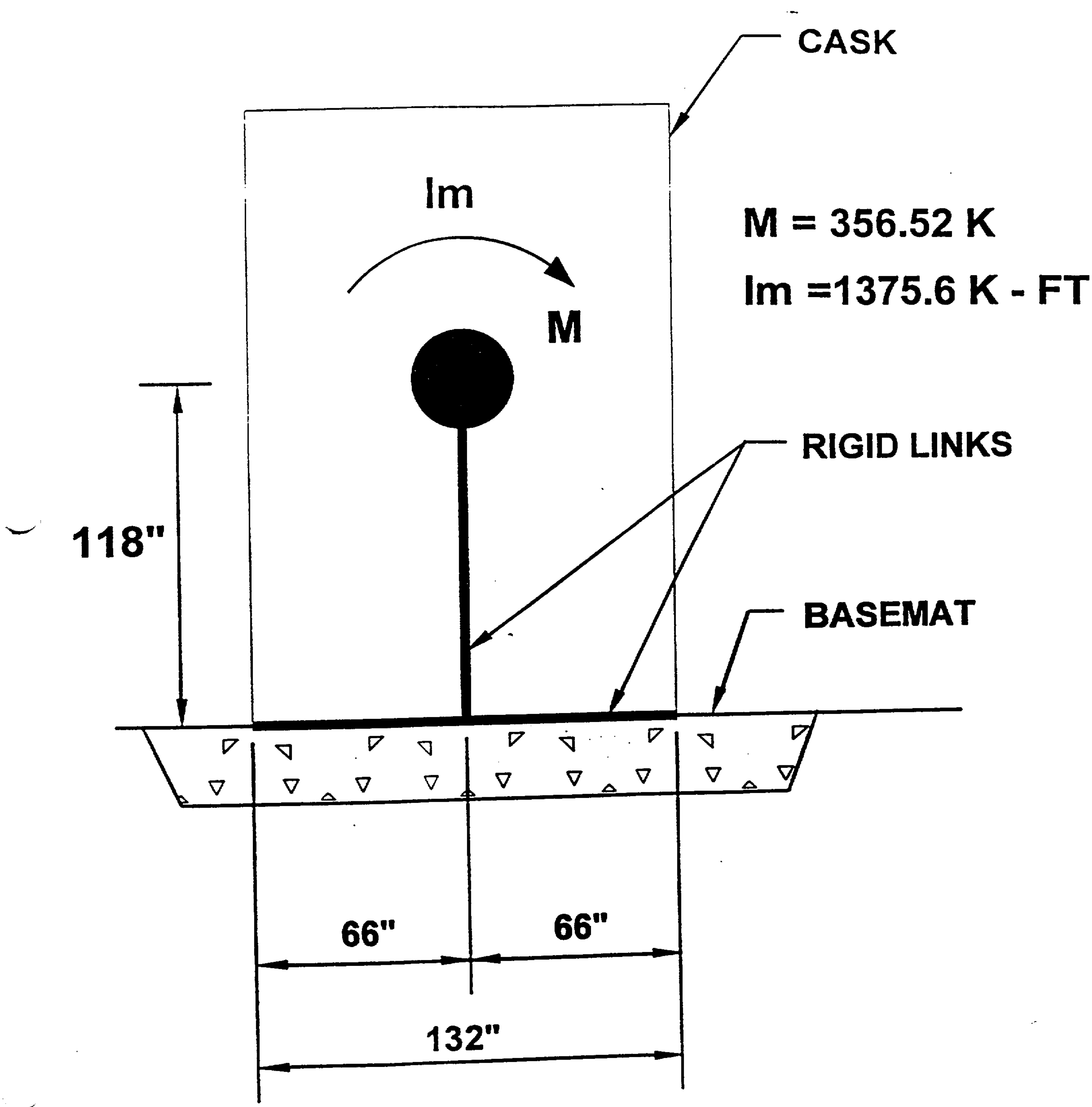


FIGURE 3.3

# SOIL-STRUCTURE INTERACTION (SSI) MOTION OF CASK - F

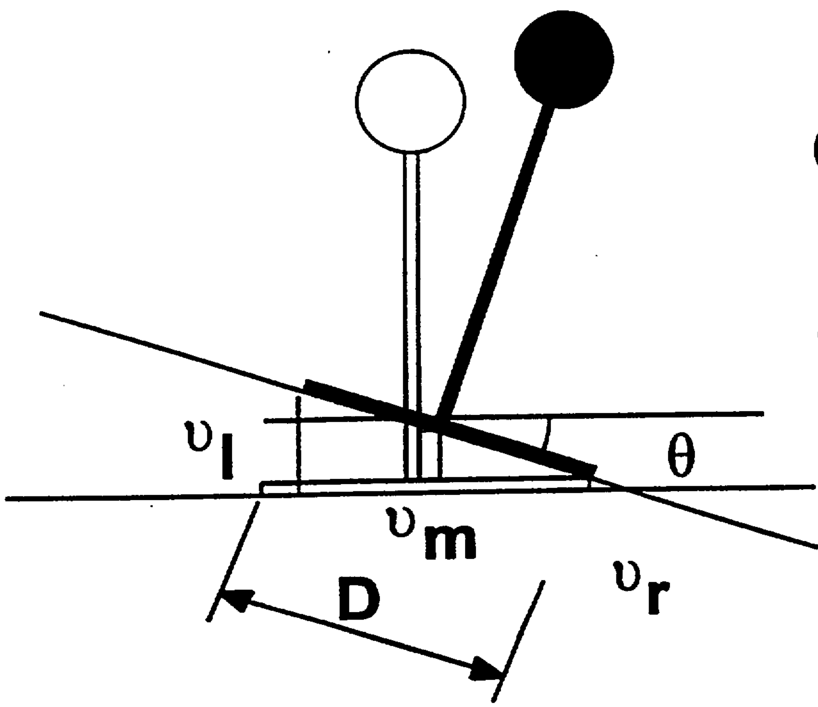


$$\theta = \frac{\upsilon_r - \upsilon_l}{D}$$

$$\upsilon = \frac{\upsilon_r + \upsilon_l}{2}$$

## CASK MOTION DUE TO SSI

FIGURE 3.4

FIGURE 3.5

**Private Storage Facility - Horiz.X-DIR.**
**Basemat, Free Field**

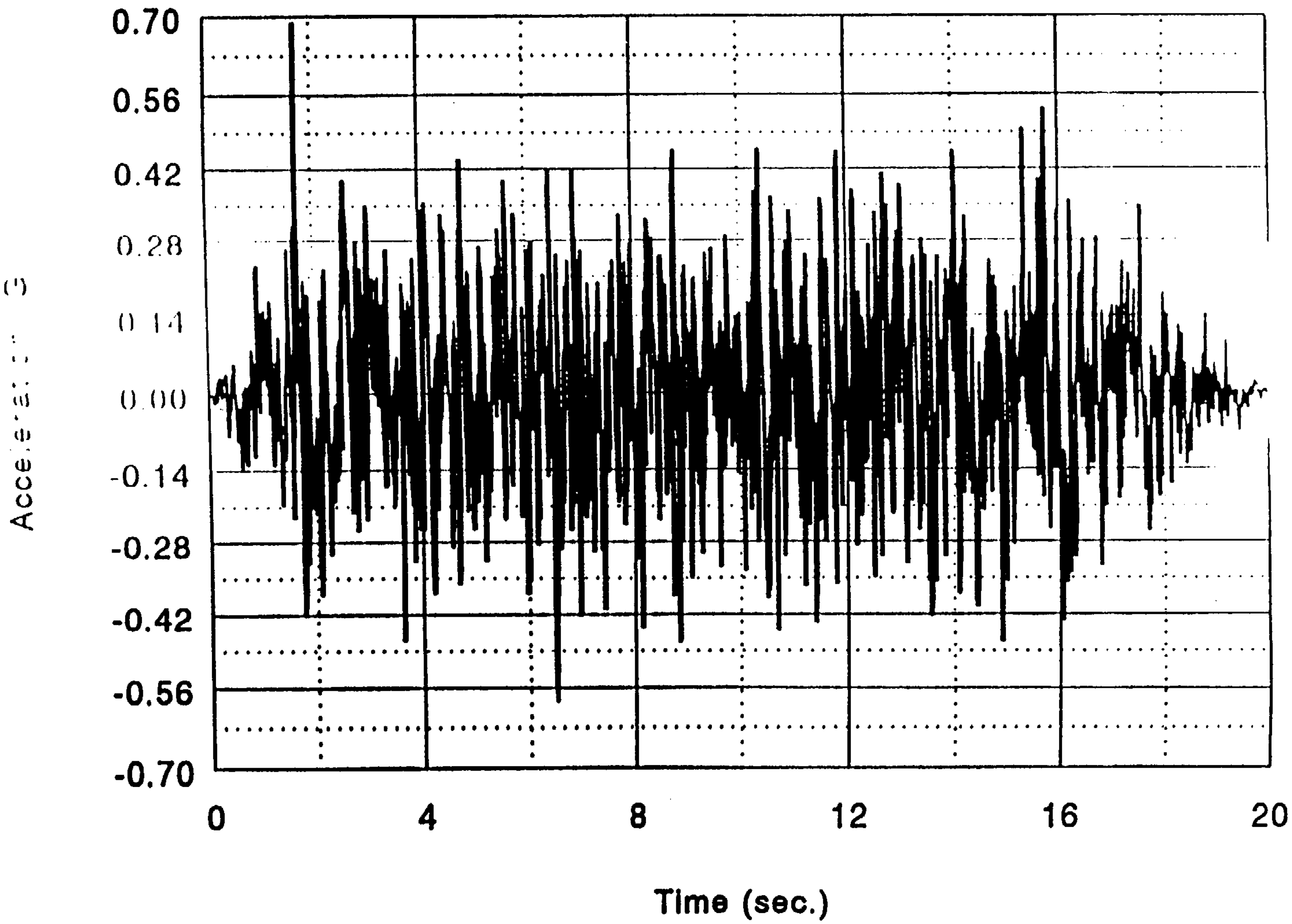

FIGURE 3.6

Private Storage Facility - Horizontal
Basemat, Node 19, X-Direction, BE

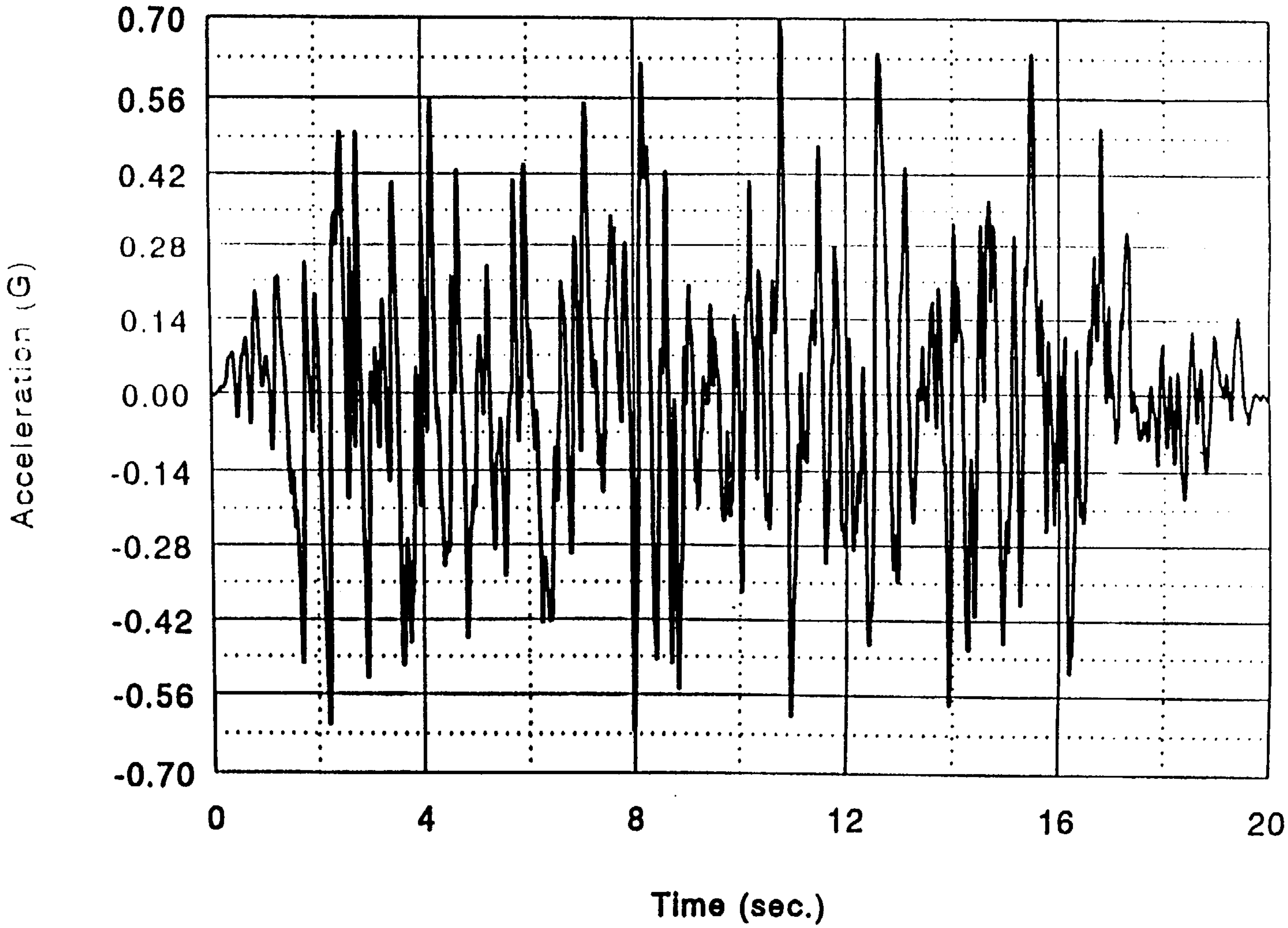

FIGURE 3.7

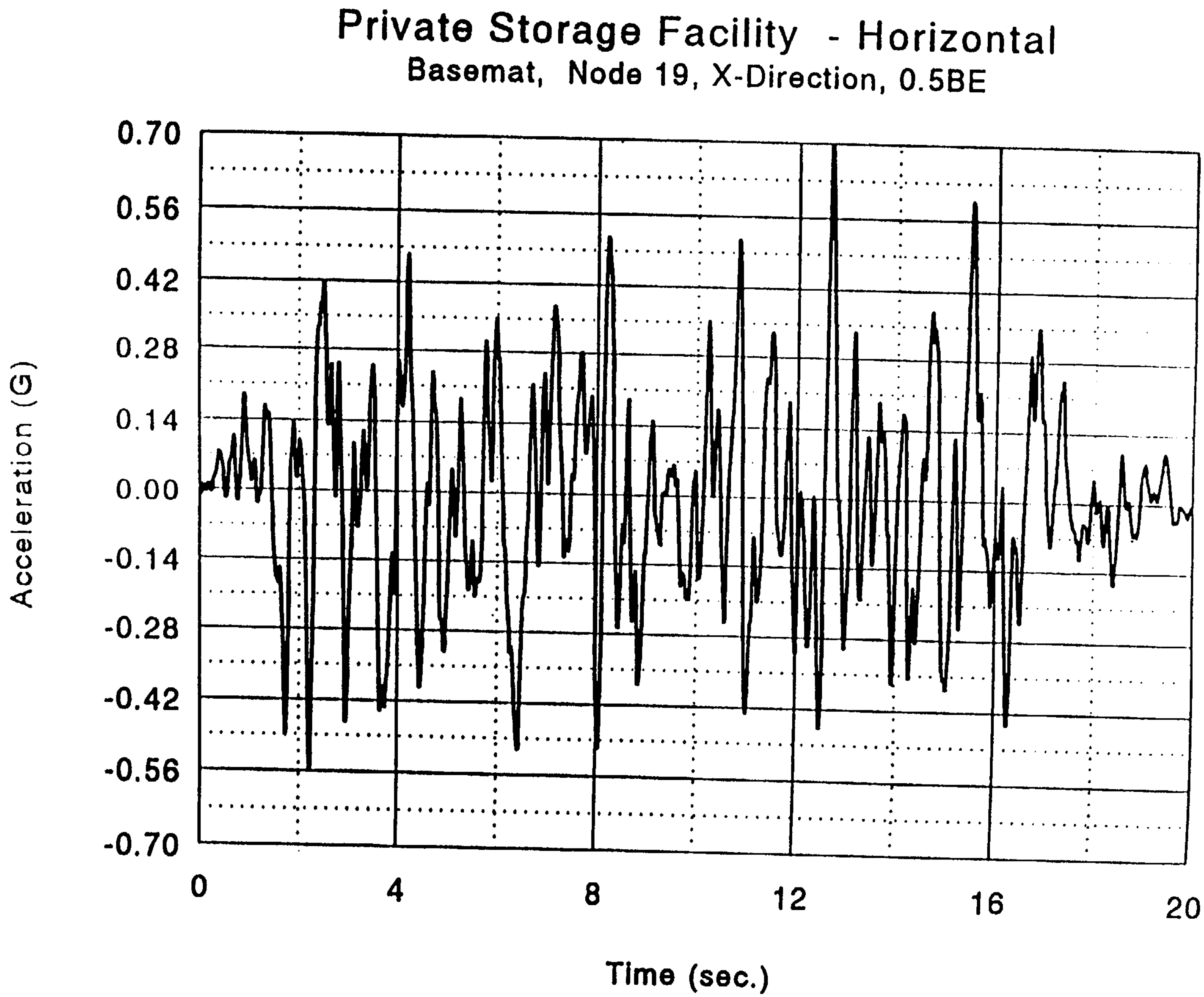
Private Storage Facility - Horizontal
Basemat, Node 19, X-Direction, 0.5BE
Acceleration (G)
0.70
0.56
0.42
0.28
0.14
0.00
-0.14
-0.28
-0.42
-0.56
-0.70
0
4
8
12
16
20
Time (sec.)

FIGURE 3.8

## Private Storage Facility - Horizontal
### Basemat, Node 19, X-Direction, 2.0BE

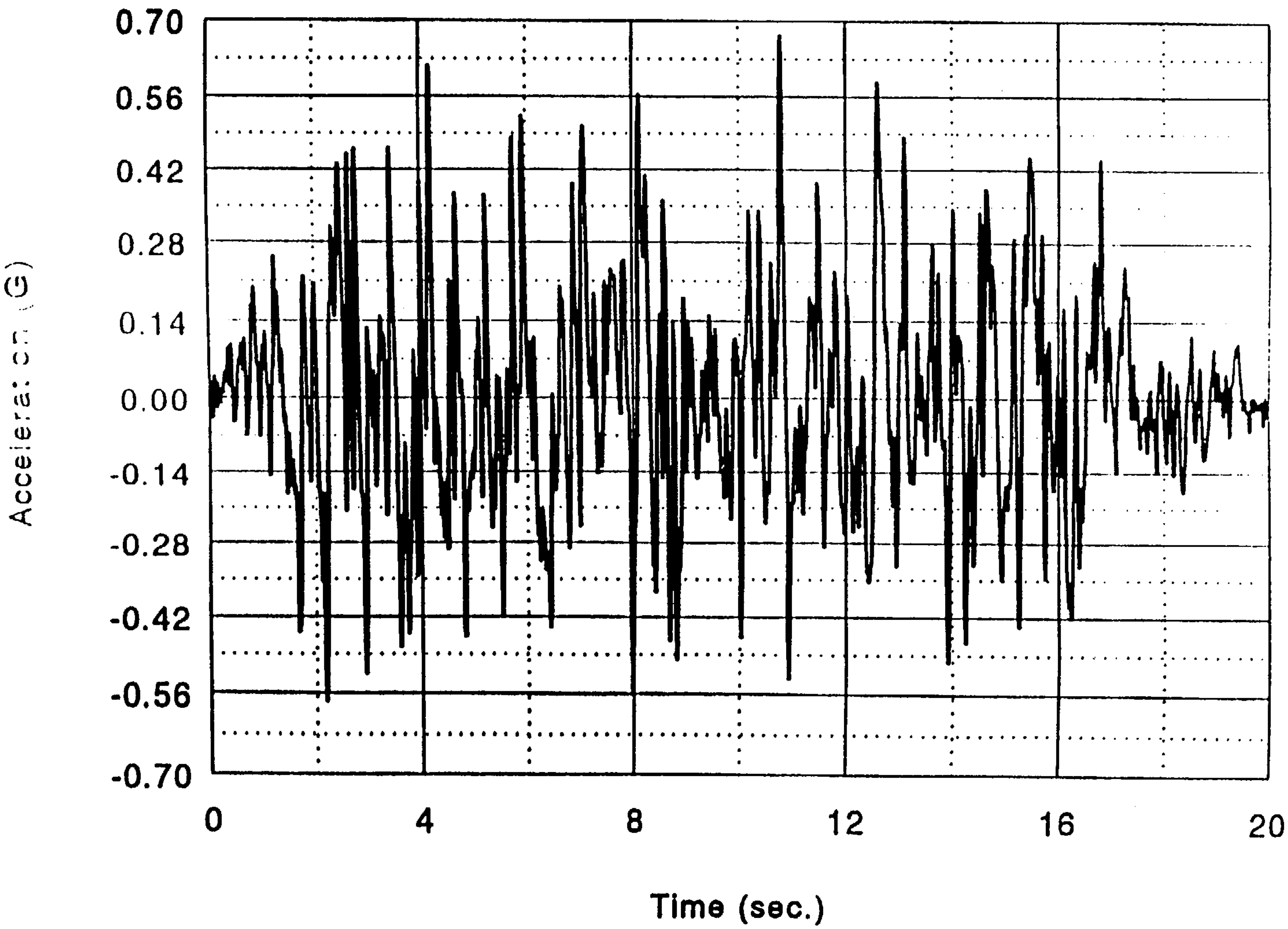

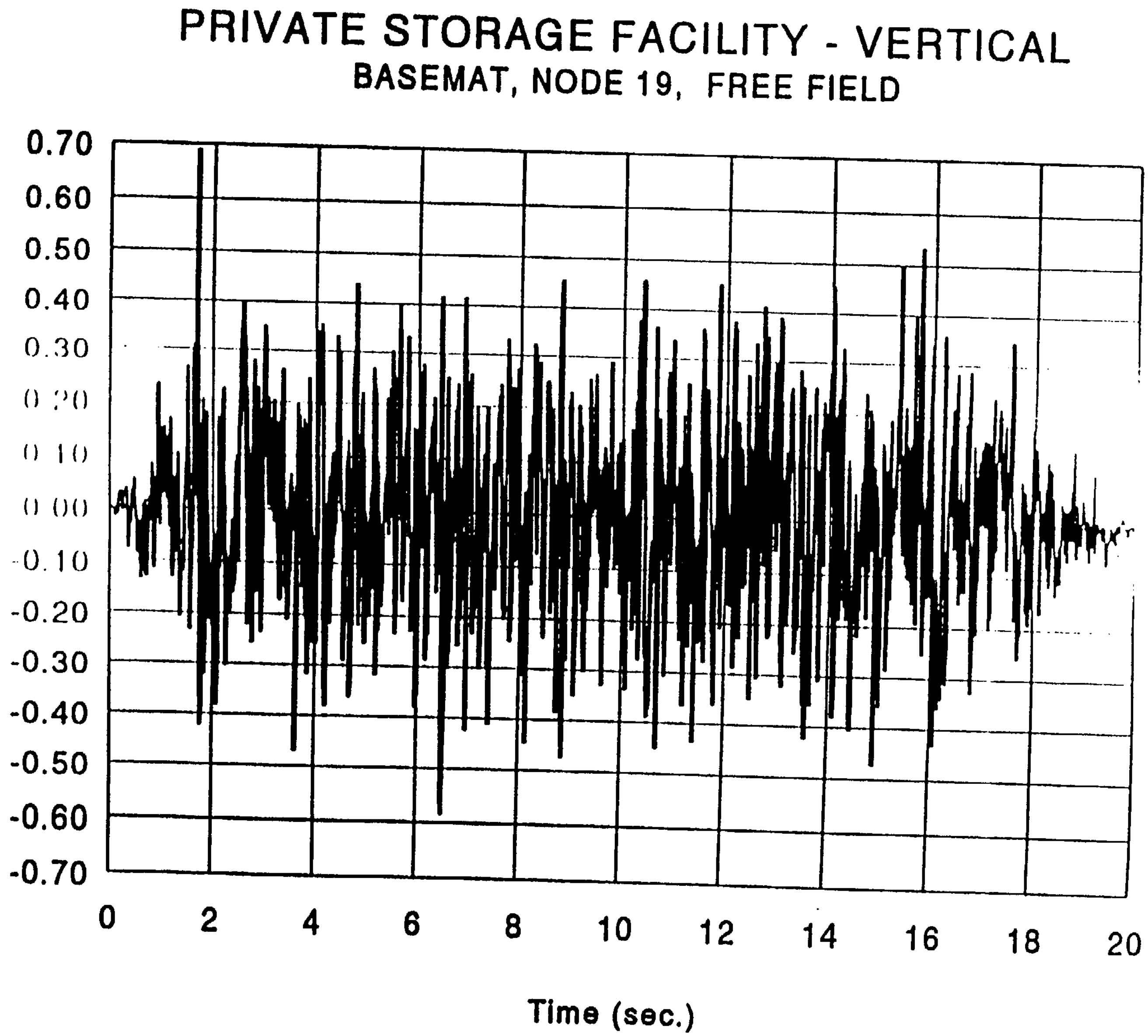
PRIVATE STORAGE FACILITY - VERTICAL
BASEMAT, NODE 19, FREE FIELD
0.70
0.60
0.50
0.40
0.30
0.20
0.10
0.00
-0.10
-0.20
-0.30
-0.40
-0.50
-0.60
-0.70
0
2
4
6
8
10
12
14
16
18
20
Time (sec.)

FIGURE 3.9

FIGURE 3.10

# PRIVATE STORAGE FACILITY - VERTICAL
## BASEMAT, NODE 19, Z-DIRECTION, BE

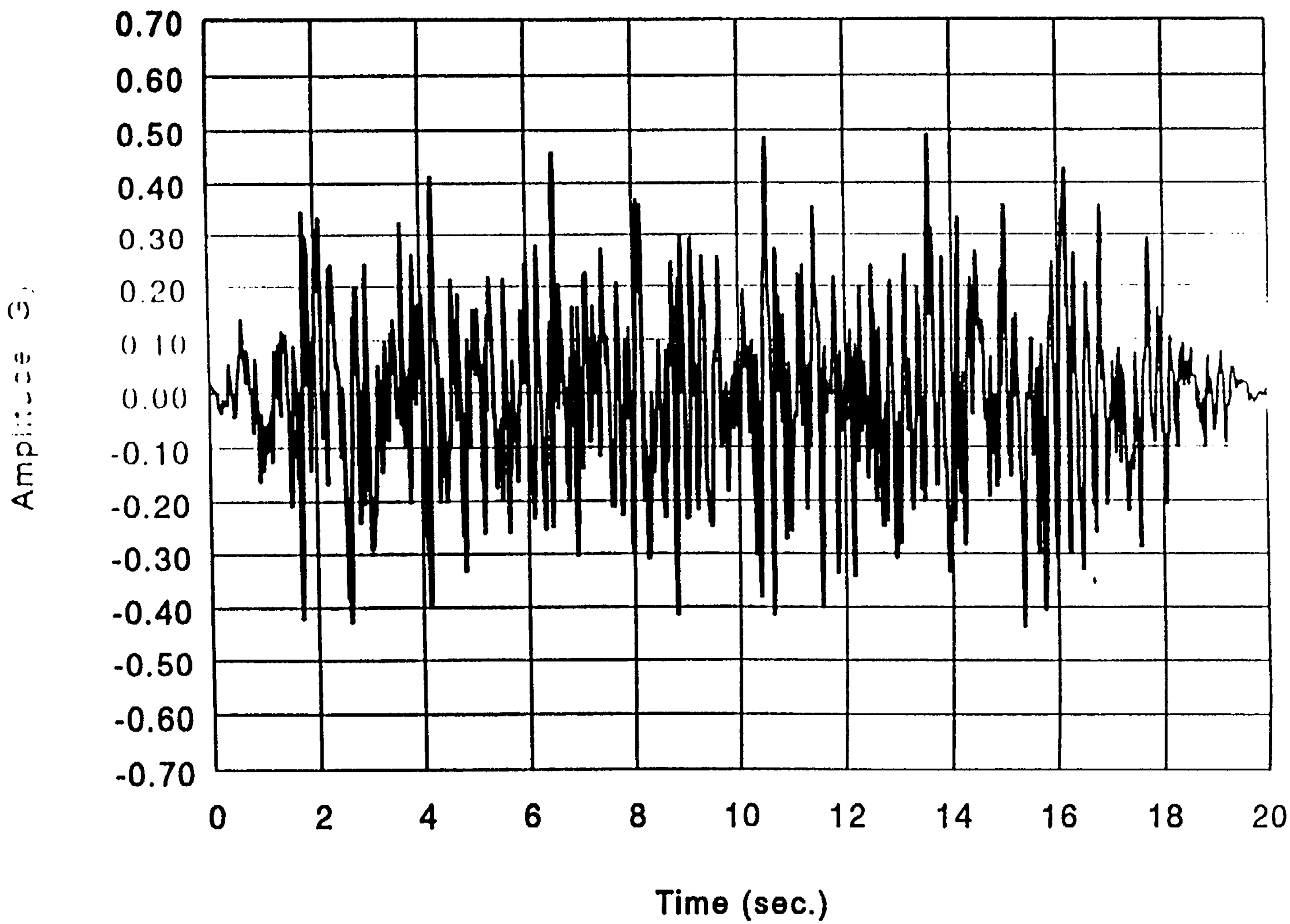

FIGURE 3.11

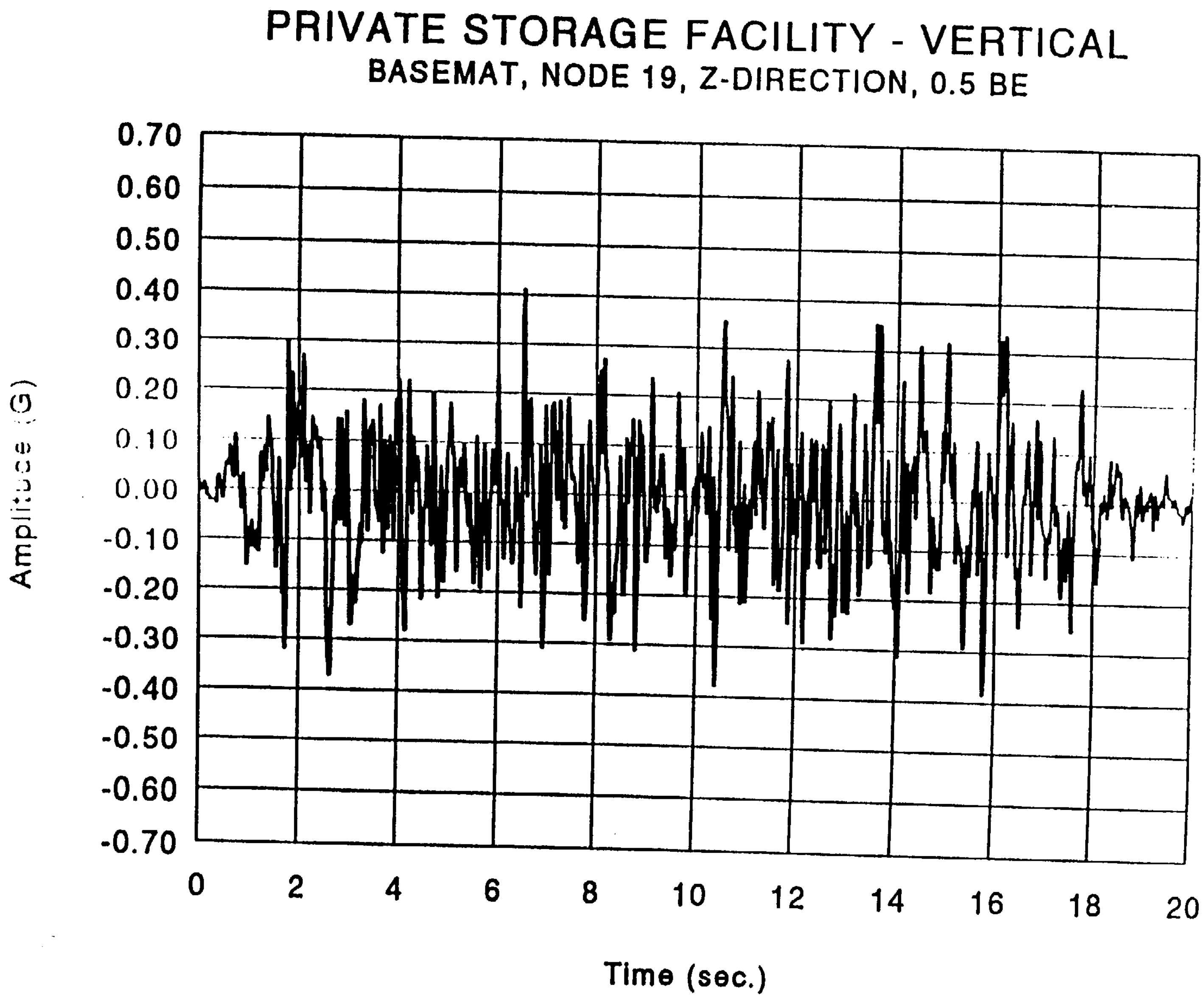

PRIVATE STORAGE FACILITY - VERTICAL
BASEMAT, NODE 19, Z-DIRECTION, 0.5 BE
0.70
0.60
0.50
0.40
0.30
0.20
0.10
0.00
-0.10
-0.20
-0.30
-0.40
-0.50
-0.60
-0.70
0
2
4
6
8
10
12
14
16
18
20
Time (sec.)

FIGURE 3.12

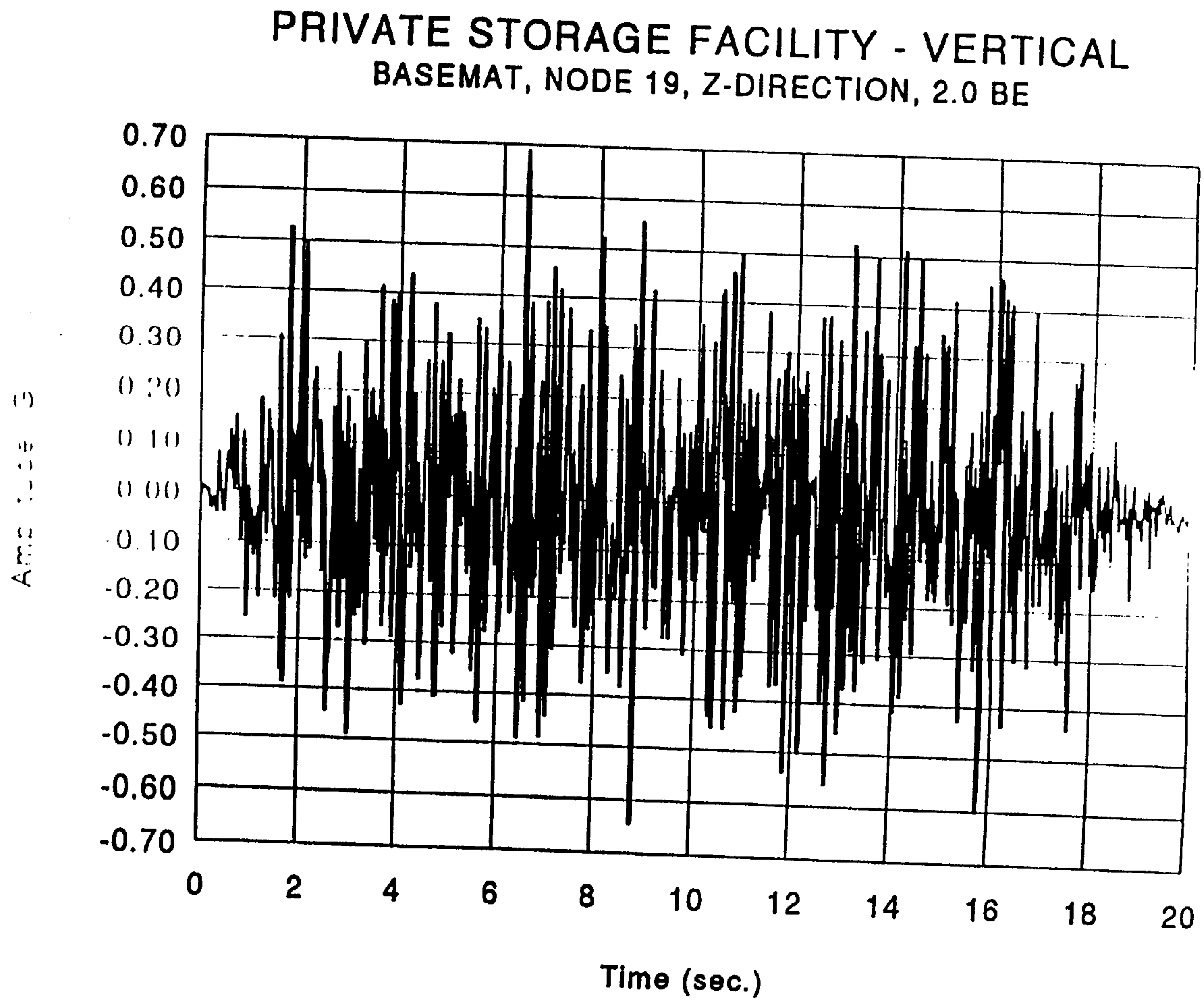
PRIVATE STORAGE FACILITY - VERTICAL
BASEMAT, NODE 19, Z-DIRECTION, 2.0 BE
0.70
0.60
0.50
0.40
0.30
0.20
0.10
0.00
-0.10
-0.20
-0.30
-0.40
-0.50
-0.60
-0.70
0
2
4
6
8
10
12
14
16
18
20
Time (sec.)

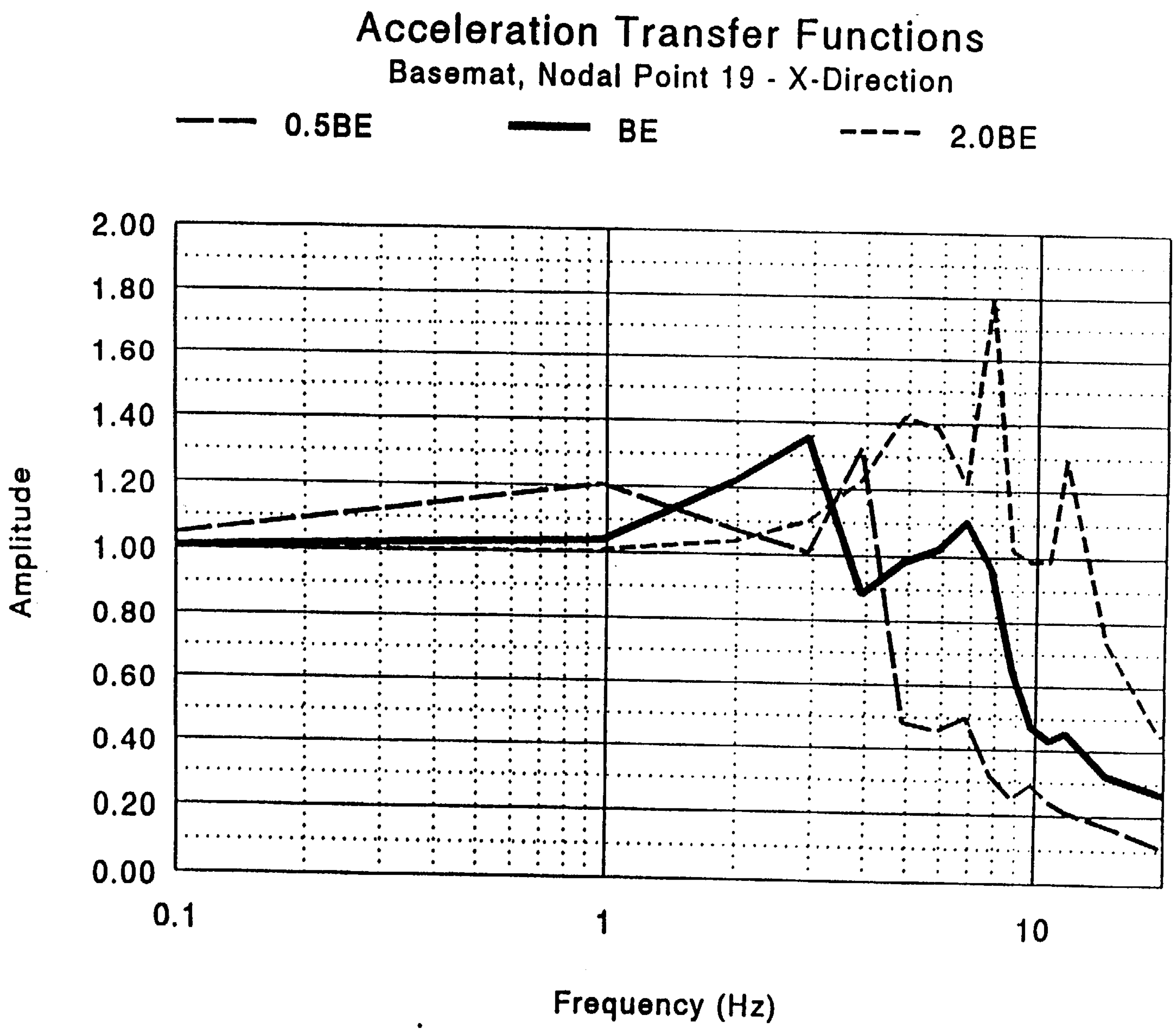
Acceleration Transfer Functions
Basemat, Nodal Point 19 - X-Direction
0.5BE
BE
2.0BE
Amplitude
2.00
1.80
1.60
1.40
1.20
1.00
0.80
0.60
0.40
0.20
0.00
0.1
1
10
Frequency (Hz)

FIGURE 3.13

FIGURE 3.14

## Acceleration Transfer Functions

### Basemat, Nodal Point 19 - Z-Direction

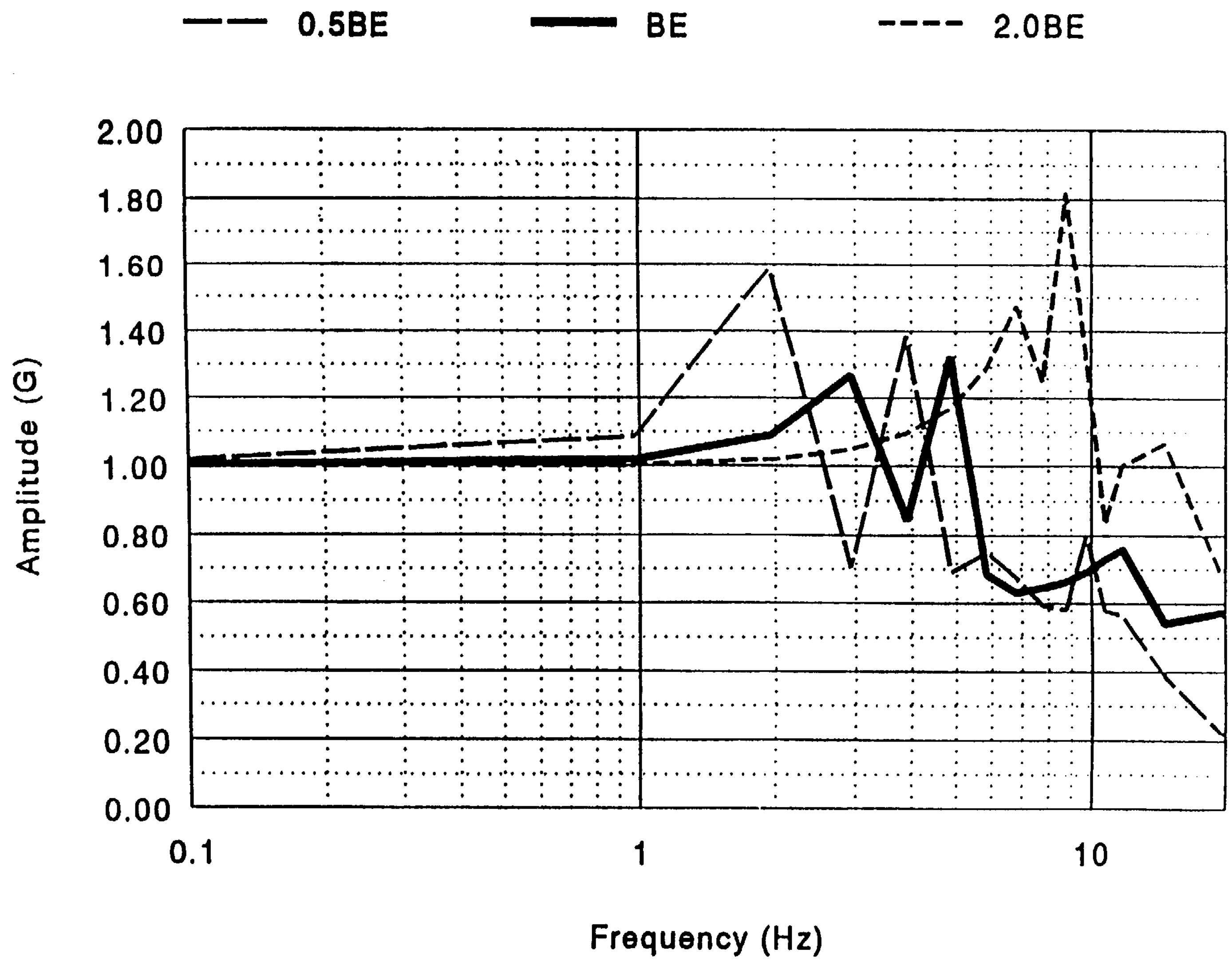

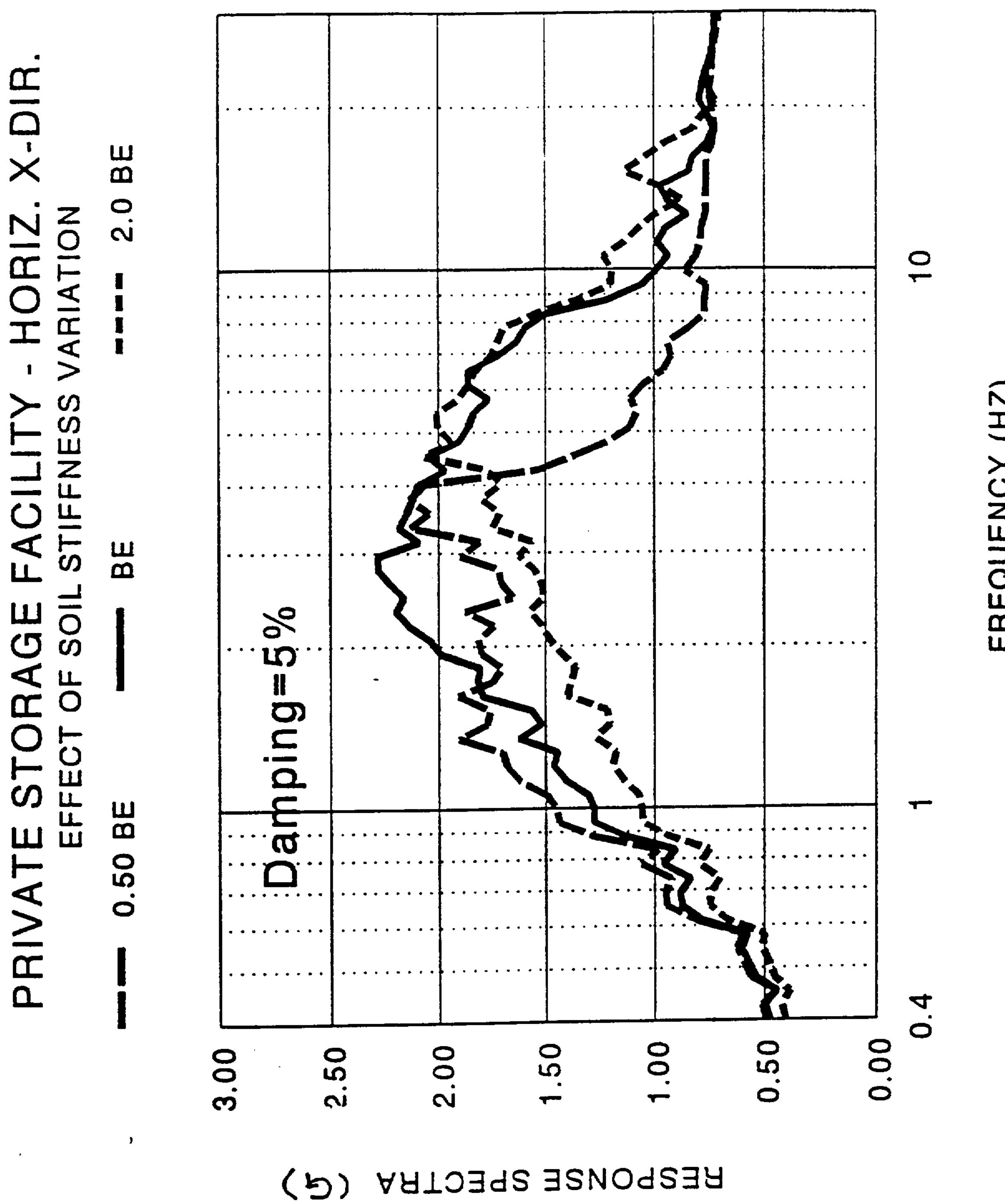


FIGURE 3.15 - Effect of Soil Stiffness Variations on Spectral Shape in X Direction at the Base of the Mat

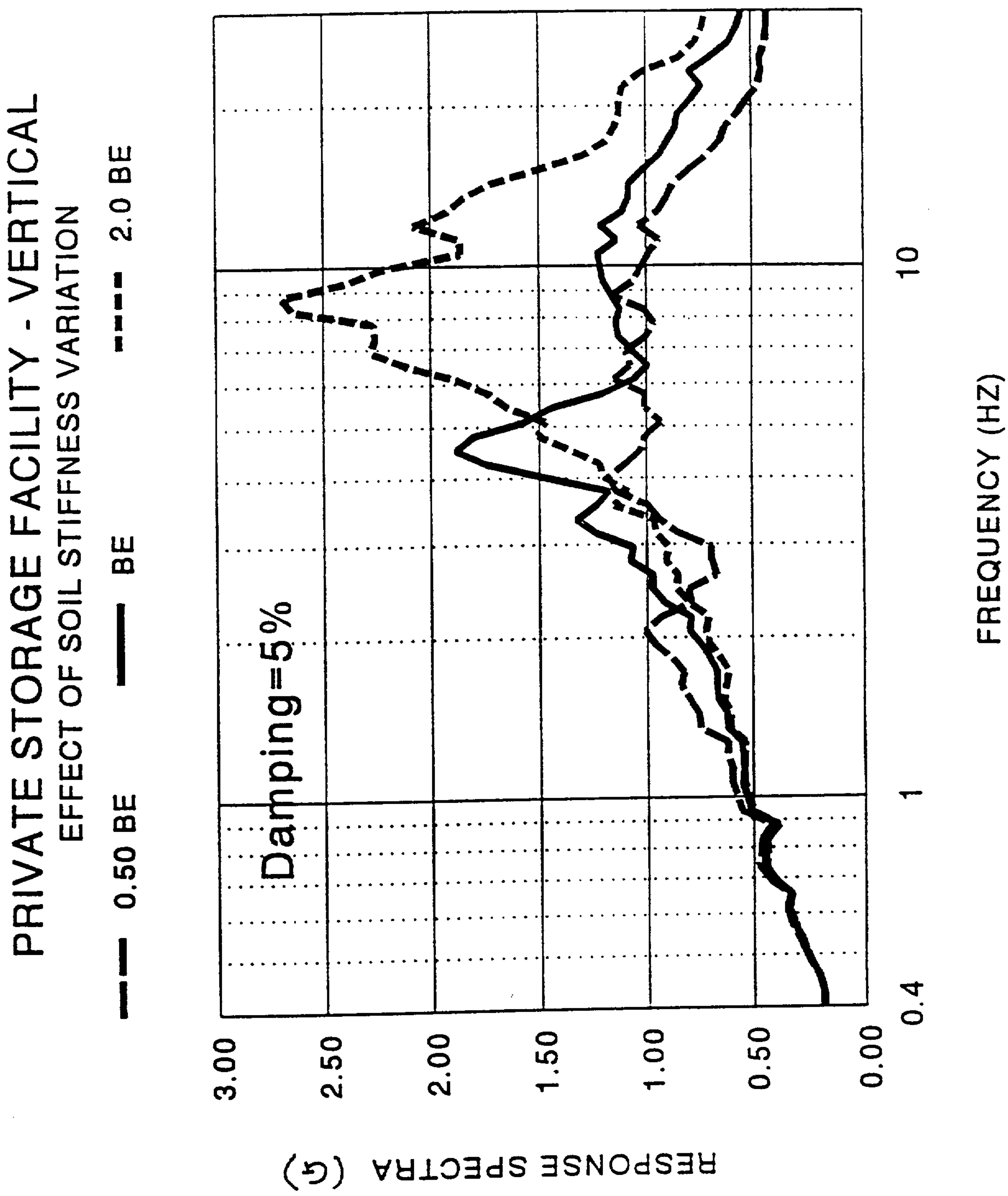


FIGURE 3.16 - Effect of Soil Stiffness Variation on Spectral Shape in the Vertical Direction at the Base of the Mat

STANSBURY 84TH-PERCENTILE SPECTRA
HORIZONTAL SPECTRAL ACCELERATIONS (G)

| PERIOD | DEEP SOIL | ROCK | ENVELOPE |
|---|---|---|---|
| 0.01 (PGA) | 0.67 | 0.67 | 0.67 |
| 0.03 | 0.67 | 0.67 | 0.67 |
| 0.05 | 0.83 | 0.87 | 0.87 |
| 0.075 | 1.05 | 1.08 | 1.08 |
| 0.1 | 1.26 | 1.27 | 1.27 |
| 0.15 | 1.47 | 1.55 | 1.55 |
| 0.2 | 1.60 | 1.63 | 1.63 |
| 0.3 | 1.65 | 1.51 | 1.65 |
| 0.5 | 1.54 | 1.16 | 1.54 |
| 0.75 | 1.34 | 0.83 | 1.34 |
| 1 | 1.13 | 0.65 | 1.13 |
| 1.5 | 0.77 | 0.42 | 0.77 |
| 2 | 0.54 | 0.30 | 0.54 |
| 3 | 0.33 | 0.17 | 0.33 |
| 4 | 0.22 | 0.11 | 0.22 |

VERTICAL SPECTRAL ACCELERATIONS (G)

| PERIOD | DEEP SOIL | ROCK | ENVELOPE |
|---|---|---|---|
| 0.01 (PGA) | 0.66 | 0.69 | 0.69 |
| 0.02 | 0.66 | -0.69 | 0.69 |
| 0.05 | 1.18 | 1.20 | 1.20 |
| 0.075 | 1.48 | 1.50 | 1.50 |
| 0.1 | 1.54 | 1.54 | 1.54 |
| 0.15 | 1.38 | 1.37 | 1.38 |
| 0.2 | 1.18 | 1.17 | 1.18 |
| 0.3 | 0.88 | 0.86 | 0.88 |
| 0.5 | 0.64 | 0.58 | 0.64 |
| 0.75 | 0.53 | 0.41 | 0.53 |
| 1 | 0.45 | 0.33 | 0.45 |
| 1.5 | 0.33 | 0.24 | 0.33 |
| 2 | 0.24 | 0.17 | 0.24 |
| 3 | 0.14 | 0.11 | 0.14 |
| 4 | 0.098 | 0.077 | 0.098 |

TABLE 3.1

Table 3.2 - Soil Dynamic Equivalent Properties

| Layer Number | Depth at Top (ft) | Soil Density (pcf) | Wave Velocity (fps) | | Material Damping (%) | |
|---|---|---|---|---|---|---|
| | | | $V_s$ | $V_p$ | $B_s$ | $B_p$ |
| 1 | 0 | 81 | 637 | 1500 | 5 | 5 |
| 2 | 2.5 | 81 | 637 | 1500 | 5 | 5 |
| 3 | 5.0 | 81 | 520 | 1500 | 10 | 10 |
| 4 | 7.5 | 81 | 520 | 1500 | 10 | 10 |
| 5 | 10.0 | 81 | 469 | 1500 | 12 | 10 |
| 6 | 12.5 | 81 | 769 | 1500 | 12 | 10 |
| 7 | 15.0 | 81 | 353 | 1500 | 15 | 10 |
| 8 | 17.5 | 81 | 353 | 1500 | 15 | 10 |
| 9 | 20.0 | 81 | 327 | 1500 | 15 | 10 |
| 10 | 22.5 | 81 | 327 | 1500 | 15 | 10 |
| 11 | 25.0 | 81 | 280 | 1500 | 15 | 10 |
| 12 | 27.5 | 81 | 280 | 1500 | 15 | 10 |
| 13 | 30.0 | 115 | 1809 | 4000 | 4 | 4 |
| 14 | 40.0 | 115 | 1809 | 4000 | 4 | 4 |
| 15 | 50.0 | 115 | 1809 | 4000 | 4 | 4 |
| 16 | 60.0 | 120 | 1861 | 4000 | 8 | 8 |
| 17 | 80.0 | 120 | 1861 | 4000 | 8 | 8 |
| 18 | 100.0 | 120 | 1861 | 4000 | 8 | 8 |
| Halfspace | 120.0 | 130 | 2080 | 5600 | 8 | 8 |

TABLE 3.2

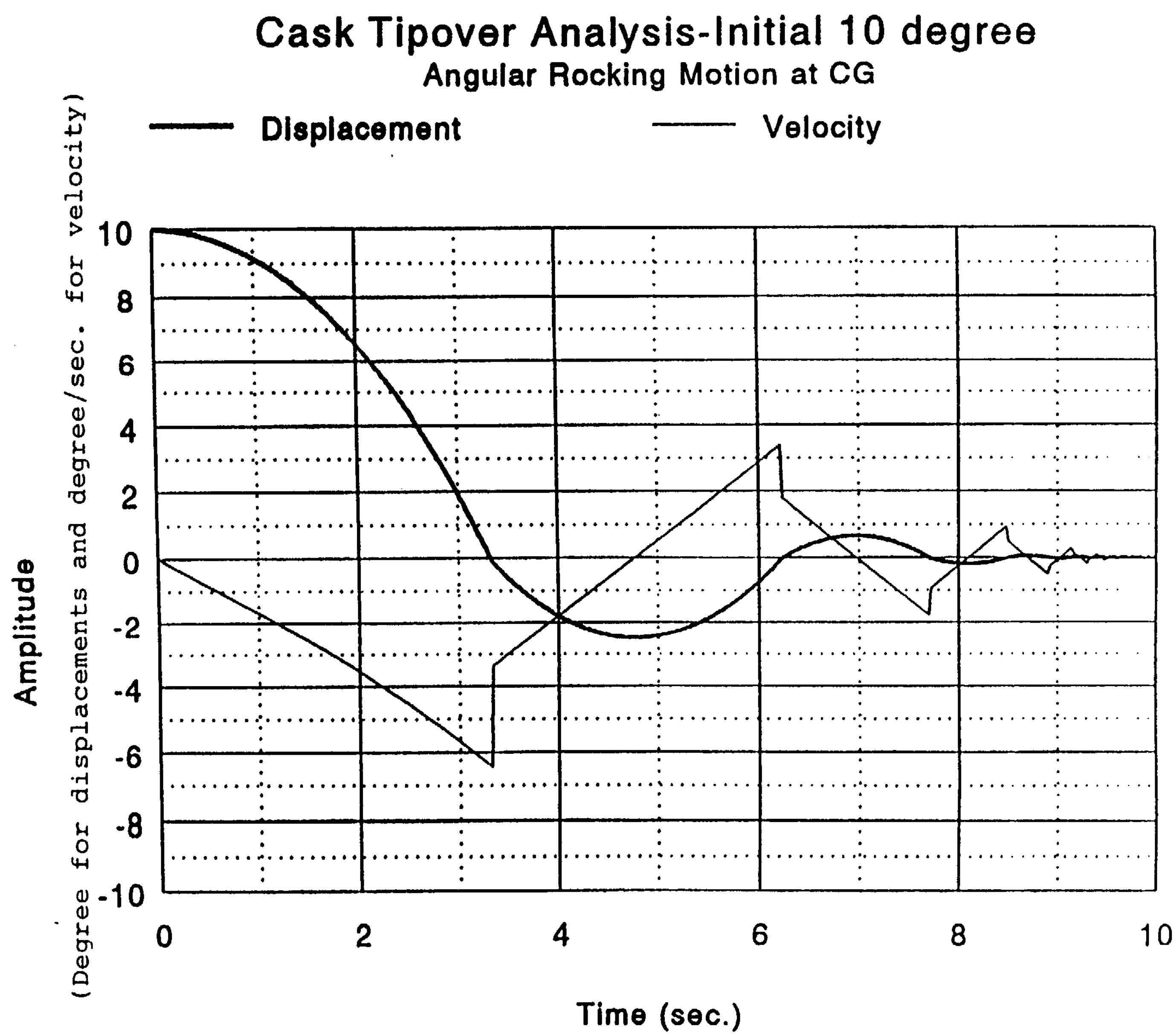


FIGURE 4.1 - Cask Tipover Motion with an Initial Rotation of 10° Including Impact

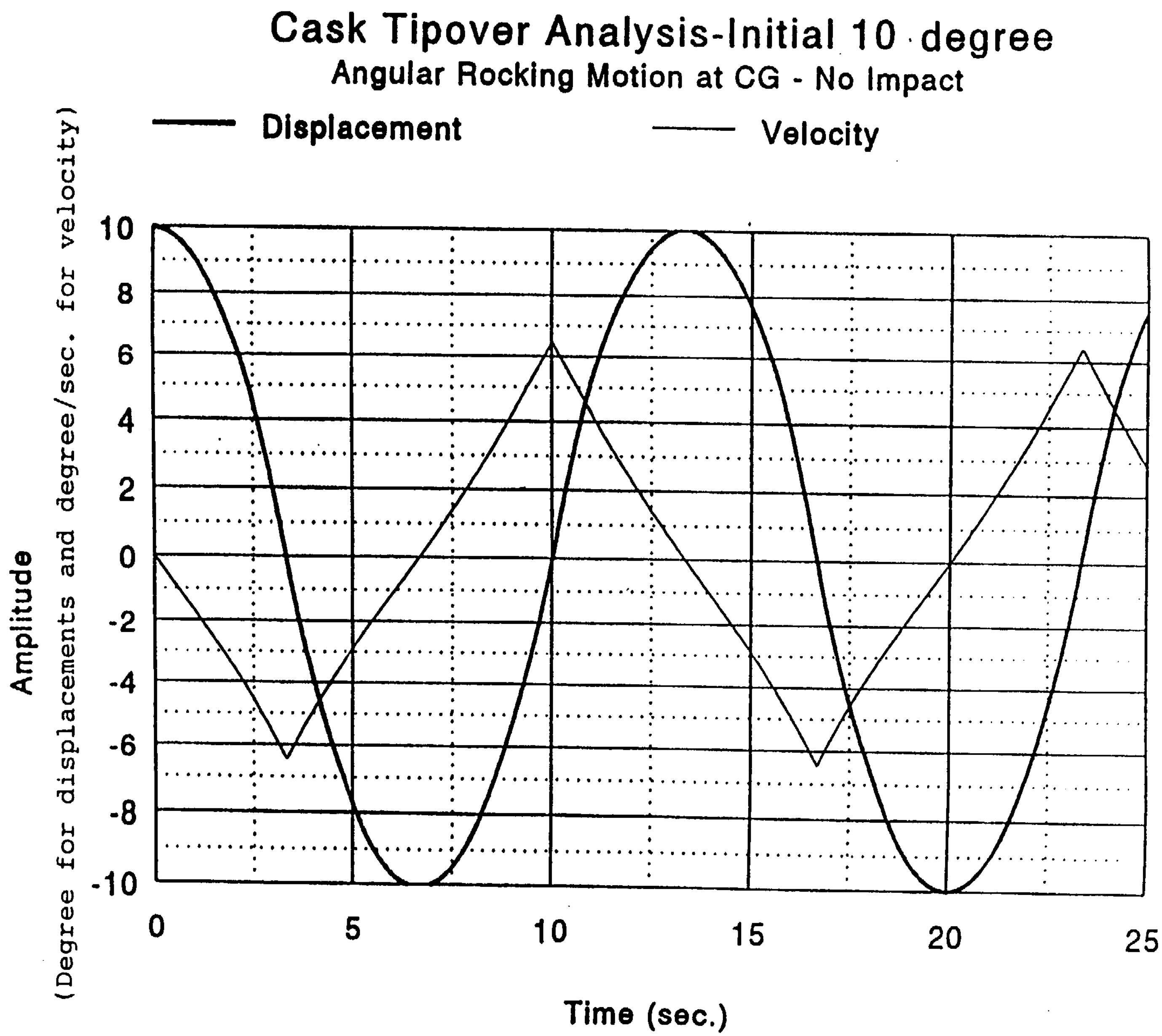


FIGURE 4.2 - Cask Tipover Motion with an Initial Rotation of 10° Without Impact

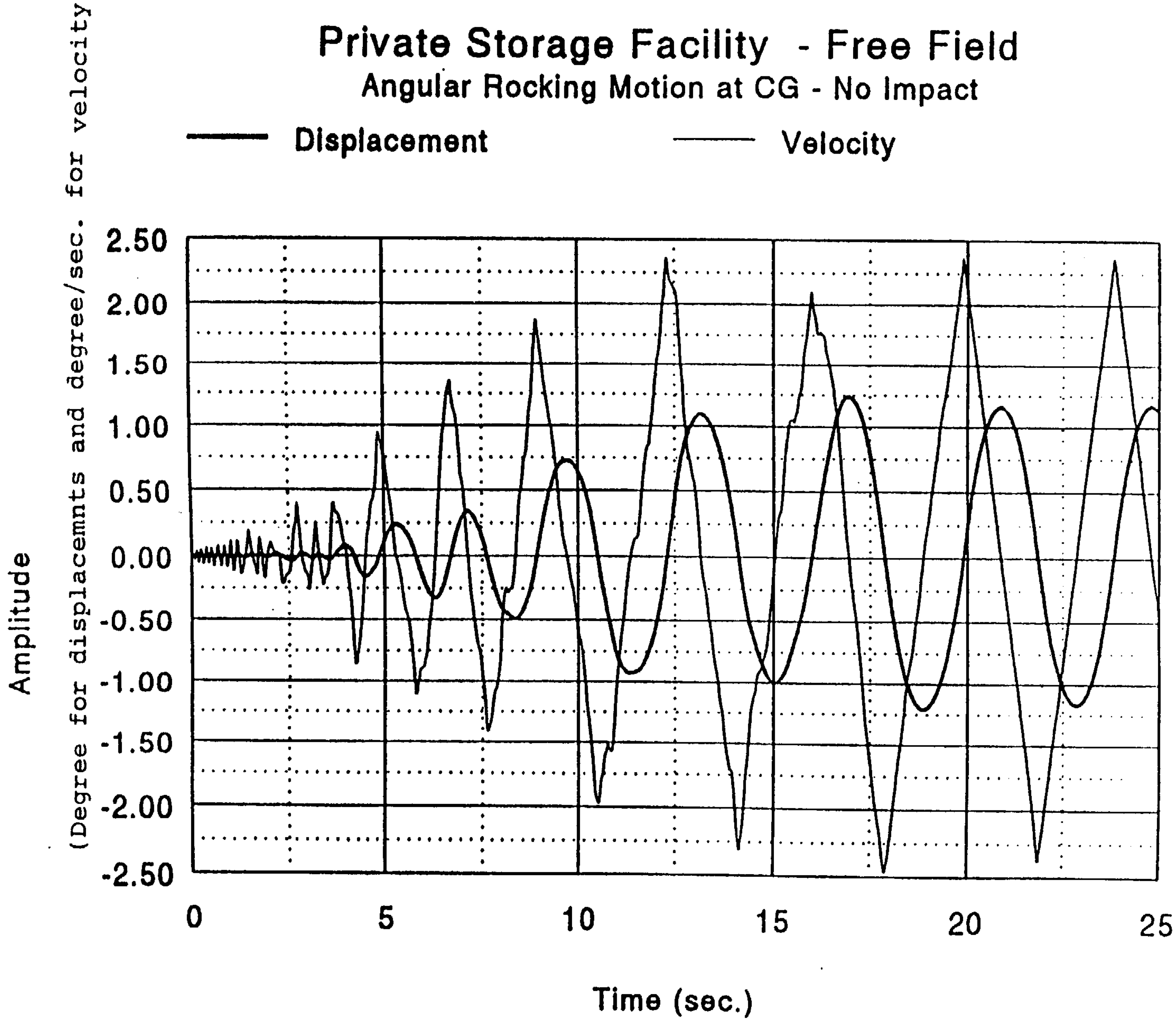


FIGURE 4.3 - Cask Rigid Body Motion Subjected to Earthquake Motion with no Impact

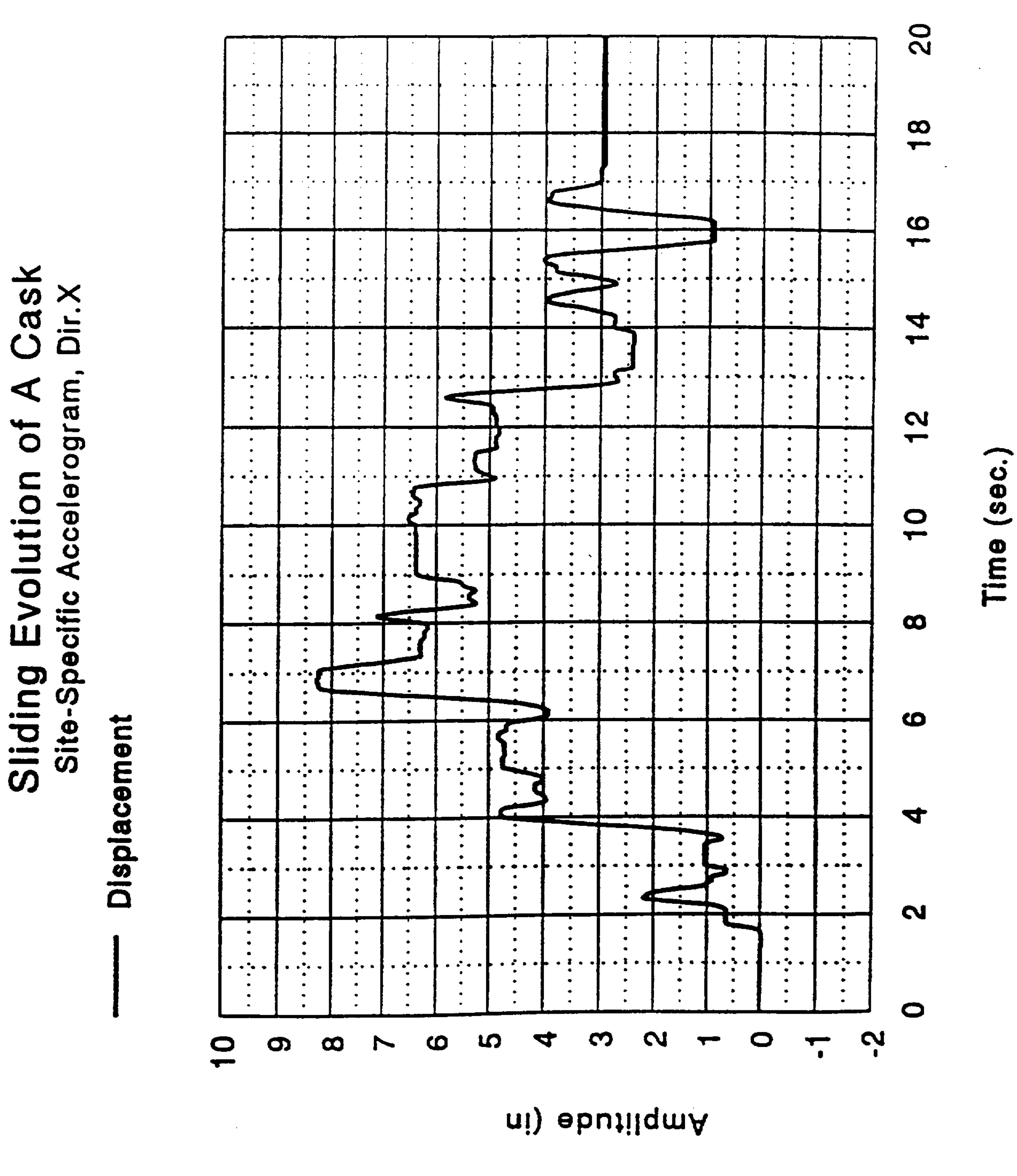


FIGURE 4.4 - Rigid Body Sliding Motion of the Cask in X Direction